

7. Eremets, M. I., Hemley, R. J., Mao, H.-K. & Gregoryanz, E. Semiconducting non-molecular nitrogen up to 240 GPa and its low-pressure stability. *Nature* **411**, 170–174 (2001).
8. Shimomura, O. *et al.* Structure analysis of high-pressure metallic state of iodine. *Phys. Rev. B* **18**, 715–719 (1978).
9. Takemura, K., Minomura, S., Shimomura, O., Fujii, Y. & Axe, J. D. Structural aspects of solid iodine associated with metallization and molecular dissociation under high pressure. *Phys. Rev. B* **26**, 998–1004 (1982).
10. Riggelman, B. M. & Drickamer, H. G. Approach to the metallic state as obtained from optical and electrical measurements. *J. Chem. Phys.* **38**, 2721–2724 (1963).
11. Sakai, N., Takemura, K. & Tsuji, K. Electrical properties of high-pressure metallic modification of iodine. *J. Phys. Soc. Jpn* **51**, 1811–1816 (1982).
12. Fujii, Y., Hase, K., Ohishi, Y., Hamaya, N. & Onodera, A. Pressure-induced monatomic tetragonal phase of metallic iodine. *Solid State Commun.* **59**, 85–89 (1986).
13. Fujii, Y. *et al.* Pressure-induced face-centered-cubic phase of monatomic metallic iodine. *Phys. Rev. Lett.* **58**, 796–799 (1987).
14. Reichlin, R. *et al.* Optical, x-ray, and band-structure studies of iodine at pressures of several megabars. *Phys. Rev. B* **49**, 3725–3733 (1994).
15. Takemura, K. Evaluation of the hydrostaticity of a helium-pressure medium with powder x-ray diffraction techniques. *J. Appl. Phys.* **89**, 662–668 (2001).
16. Yamamoto, A. *et al.* Rietveld analysis of the modulated structure in the superconducting oxide $\text{Bi}_2(\text{Sr,Ca})_2\text{Cu}_2\text{O}_{8+x}$. *Phys. Rev. B* **42**, 4228–4239 (1990).
17. Wilson, A. J. C. & Prince, E. (eds) *International Tables for Crystallography Vol. C*, 2nd edn, 914–926 (Kluwer Academic, Dordrecht, 1999).
18. Luty, T. & Raich, J. C. Molecular to atomic transformation in solid iodine under high pressure. *Can. J. Chem.* **66**, 812–818 (1988).
19. Nelmes, R. J., Allan, D. R., McMahon, M. I. & Belmonte, S. A. Self-hosting incommensurate structure of barium IV. *Phys. Rev. Lett.* **83**, 4081–4084 (1999).
20. Fujihisa, H., Fujii, Y., Takemura, K. & Shimomura, O. Structural aspects of dense solid halogens under high pressure studied by x-ray diffraction—molecular dissociation and metallization. *J. Phys. Chem. Solids* **56**, 1439–1444 (1995).
21. Fujii, Y. *et al.* Evidence for molecular dissociation in bromine near 80 GPa. *Phys. Rev. Lett.* **63**, 536–539 (1989).
22. Takemura, K., Sahu, P. Ch., Kunii, Y. & Toma, Y. Versatile gas-loading system for diamond-anvil cells. *Rev. Sci. Instrum.* **72**, 3873–3876 (2001).
23. Zha, C.-S., Mao, H.-K. & Hemley, R. J. Elasticity of MgO and a primary pressure scale to 55 GPa. *Proc. Natl Acad. Sci. USA* **97**, 13494–13499 (2000).
24. Shimomura, O. *et al.* Application of an imaging plate to high-pressure X-ray study with a diamond anvil cell. *Rev. Sci. Instrum.* **63**, 967–973 (1992).
25. Takemura, K. & Nakano, S. Performance of a synthetic diamond-backing plate for the diamond-anvil cell at ultrahigh pressures. *Rev. Sci. Instrum.* **74**, 3017–3020 (2003).

Acknowledgements We thank A. Yamamoto for the use of his programs for the analysis of the modulated structure, and O. Mishima for comments. The synchrotron radiation experiments were performed with the approval of the Photon Factory.

Competing interests statement The authors declare that they have no competing financial interests.

Correspondence and requests for materials should be addressed to T.K. (takemura.kenichi@nims.go.jp).

Gigantic jets between a thundercloud and the ionosphere

H. T. Su*†, R. R. Hsu*†, A. B. Chen†, Y. C. Wang†, W. S. Hsiao†, W. C. Lai†, L. C. Lee†‡, M. Sato§ & H. Fukunishi§

† Department of Physics, National Cheng Kung University, Tainan, 70148, Taiwan

‡ National Space Program Office, Hsin-Chu, 30077, Taiwan

§ Department of Geophysics, Tohoku University, Sendai 980-8578, Japan

* These authors contributed equally to this work

Transient luminous events in the atmosphere, such as lightning-induced sprites^{1–8} and upwardly discharging blue jets^{9–14}, were discovered recently in the region between thunderclouds and the ionosphere. In the conventional picture, the main components of Earth's global electric circuit^{15,16} include thunderstorms, the conducting ionosphere, the downward fair-weather currents and the conducting Earth. Thunderstorms serve as one of the generators that drive current upward from cloud tops to the ionosphere, where the electric potential is hundreds of kilovolts higher than Earth's surface. It has not been clear, however,

whether all the important components of the global circuit have even been identified. Here we report observations of five gigantic jets that establish a direct link between a thundercloud (altitude ~16 km) and the ionosphere at 90 km elevation. Extremely-low-frequency radio waves in four events were detected, while no cloud-to-ground lightning was observed to trigger these events. Our result indicates that the extremely-low-frequency waves were generated by negative cloud-to-ionosphere discharges, which would reduce the electrical potential between ionosphere and ground. Therefore, the conventional picture of the global electric circuit needs to be modified to include the contributions of gigantic jets and possibly sprites^{17,18}.

On the evening of 22 July 2002, an oceanic thunderstorm system was seen raging over the South China Sea near Luzon Island, Philippines (Fig. 1). Low-light-level cameras were set up at Kenting, which is located at the southern tip of Taiwan, to observe this thunderstorm. Between 14:09 and 14:21 UT, five gigantic optical jets were recorded above the thundercloud. At the fully developed stage, events 1 (Fig. 2) and 5 had a tree-shaped upper part and a blue-jet-like lower section, and hence are called 'tree' jets. For events 2, 3, 4 (Fig. 3), the upper section looked like a carrot, the lower section resembled a blue jet, and these are called 'carrot' jets.

Using the star field as a guide, the lines of sight of these events were found to intercept the convective core of the thundercloud. The obstructive low clouds (Figs 2 and 3) indicated that the gigantic jets emerged from the convective core, not from the front edge of the thundercloud. At this range, the corresponding heights of these jets were 90 ± 5 km (event 1), 89 ± 5 km (event 2), 86 ± 5 km (event 3), 91 ± 5 km (event 4) and 91 ± 5 km (event 5). All events reached

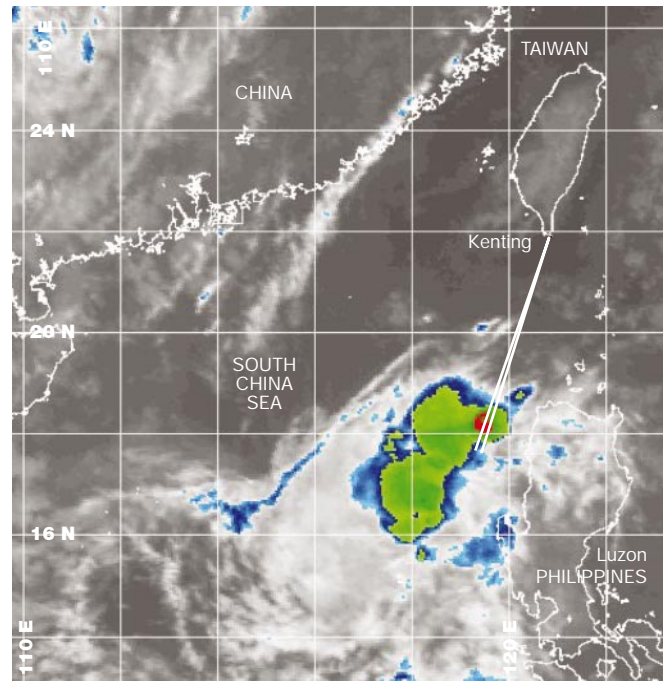


Figure 1 Infrared cloud map near Taiwan taken by the GMS 5 satellite at 14:31 UT, 22 July 2002. The occurrence times of five gigantic jets were 14:09:18 UT (event 1), 14:11:59 UT (event 2), 14:15:15 UT (event 3), 14:20:01 UT (event 4) and 14:20:54 UT (event 5). The two white lines represent the range of the line-of-sight extending from the observation site (at Kenting, Taiwan) to the centre of a gigantic jet. The convective core of the thunderstorm (red colour) is at a distance of 440 ± 20 km from Kenting. The colours on the infrared map represent the temperature and height of clouds, with red indicating the coldest and highest region. The cloud top inferred from the temperature profile is 16 km for the convective core.

the ionosphere, which has a night-time ionization starting at 80 km height and reaching the first peak density at 110 km, based on the International Reference Ionosphere (IRI-95) model¹⁹.

From the recorded images, the apparent emerging point of the jets was at 18 km height for event 2, which is only 2 km higher than the inferred cloud-top (16 km). For the jets shown in Figs 2 and 3, the apparent emerging points were 22 km and 24 km. The variation in emerging height was due to movement of the front cloud gap. Thus, these gigantic jets originated at the top of the convective core, and reached an elevation of 90 km in the ionosphere.

The images in Figs 2 and 3 are selected to illustrate the dynamical behaviours of the gigantic jets. The luminous duration was ~417 ms for event 1 (Fig. 2) and ~650 ms for event 4 (Fig. 3). The evolution of gigantic jets consists of three stages: leading jet, fully developed jet, and trailing jet. The propagating speed of the leading jets was ~1,000 km s⁻¹ for event 1 and ~1,200 km s⁻¹ for event 4. Both leading jets lasted only for two fields (each field is 17 ms). The form and evolution of the leading jets are similar to the blue jet recorded by Pasko *et al.*¹⁴, but had a much shorter duration. The propagation velocities of the leading jets reported here are an order of magnitude higher than those of classical blue jets and Pasko's jet, but are comparable to the velocities of stepped leaders in conventional cloud-to-ground lightning (CG)^{20,21}.

The fully developed jets lasted for less than 17 ms (Fig. 2) and for 167 ms (Fig. 3). At this stage, each gigantic jet appears to be a hybrid of sprite and blue jet, with its upper section, lower section, and apparent emerging point brightening concurrently. This feature is

similar to the return stroke in a CG^{20,21}, and the radio data, to be presented later, seem to support this assessment.

In Fig. 2, the trailing jet (field 5 and onward) was seen to rush upward with a speed of 26 km s⁻¹, and terminated at an elevation of ~60 km. The trailing jet lasted for 233 ms. After the trailing jet disappeared, the apparent emerging point re-brightened 17 ms later and lasted for two fields. The trailing jet in Fig. 3 propagated upward with a velocity of 120 km s⁻¹. As the trailing jet approached 60 km in elevation, its speed slowed down to 13 km s⁻¹ and it finally stopped at ~68 km. The persisting time of the trailing jet was 367 ms. The apparent emerging point also exhibited a re-brightening 167 ms later, and lasted for only one field. The trailing jets in all five events assume a conic shape with a ~25° conic angle, similar to the turbulence jet emerging from a nozzle²².

During this observation, synchronization of the recorder clock to global positioning system (GPS) time was done manually, and the time accuracy of the events was about a second. The uncertainty in time accuracy will not affect the results presented so far. But it did impose some difficulties when trying to correlate these optical events with CGs and extremely-low-frequency (ELF) transients.

From the ELF transients recorded by Onagawa station in Japan (Fig. 4) and Syowa station in Antarctica, a one-to-one match of the ELF event²³ to the jet was found for events 1, 2, 4 and 5. The ELF waves in all four cases have a polarization as generated by positive

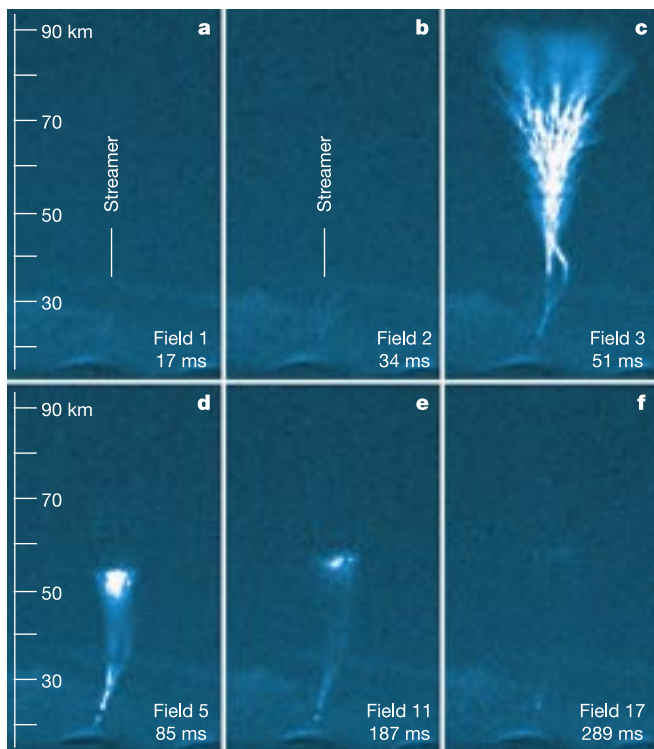


Figure 2 Selected and cropped image fields of event 1. The monochrome images were tinted to various shades of blue to bring out the salient structural features. The imaging system consists of a Watec N-100 CCD, a 20 mm/f1.8 lens, and a digital video recorder. Frame rate of the imaging system is 30 frames per second. Each frame was further separated into even and odd image fields of ~17-ms resolution. The spectral sensitivity of the CCD is from 400 to 1,000 nm, with 50% detection efficiency at 400 nm and at 780 nm. The persistent time of the Watec CCD's phosphor is less than 0.01 ms. (The cameras we used are intensified low light level cameras, which used a phosphor coating as image intensifier.)

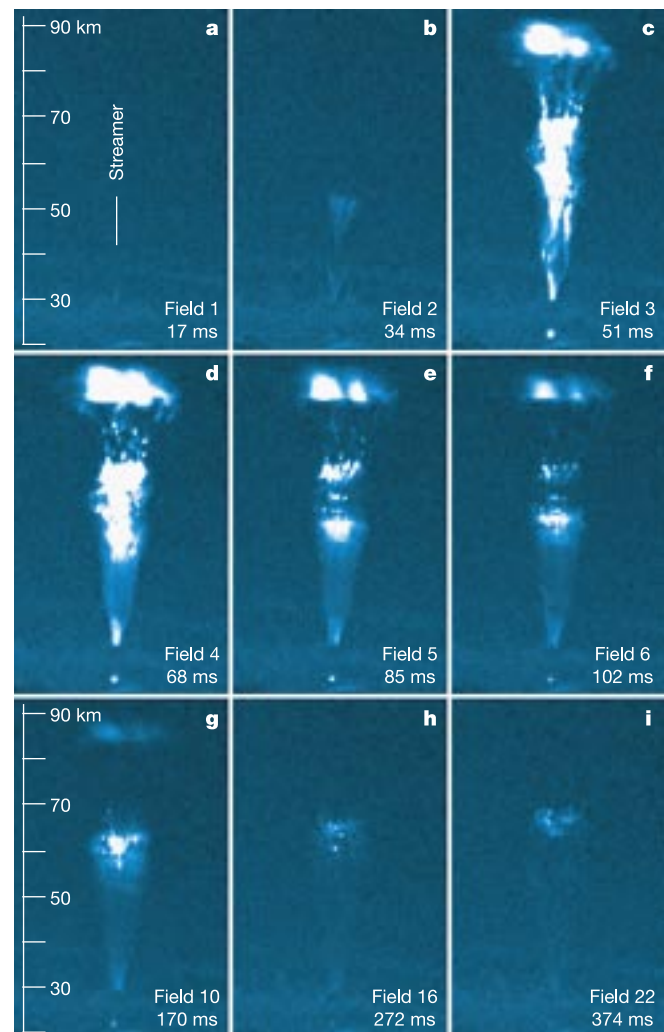


Figure 3 Selected and cropped image fields of event 4. The gigantic jet evolves in three stages: the leading jet (a, b), the fully developed jet (c-g) and the trailing jet (e-i).

CG (+CG) lightning. To locate the causative ELF sources, we performed triangulations¹⁷ using the data from the two ELF stations. The uncertainty in the ELF geolocating method is approximately 1,500 km. The results put one of the ELF causative sources in the general area of the jet-producing thunderstorm. However, the ELF transient time lagged behind the time of the optical event at the fully developed stage by 1.03, 1.01, 1.07 and 1.06 seconds. We believe these consistent time lags indicate that the recorder clock led the GPS clock of the ELF stations by about a second. Therefore, these four tree and carrot jets have their associated ELF transients. The charge moment changes¹⁸ inferred from ELF data were 1,700 and 2,000 C km for the two tree jets (events 1 and 5), and 1,000 C km for the two carrot jets (events 2 and 4). The difference in the charge moment change is consistent with the morphological difference of tree and carrot jets. A possible ELF transient for event 3 was found with a time lag of 0.59 seconds. Furthermore, the ELF geolocation puts the causative sources near Africa or North America. Therefore, no ELF was associated with this event.

Knowing the corrected times of optical jets, we can look for possible triggering CGs. We found no discernible lightning flash that preceded these gigantic jets. Next we examined data recorded by the TOGA lightning detection network²⁴, which operates in the western Pacific Rim. The TOGA network has a 10,000-km detection range and a 2-km positioning accuracy. We found no CGs that were close in time and in position to the jets. However, CGs could elude the detection of TOGA network when their current rise time was longer than 22 μ s. This feature is similar to classic blue-jet events^{11–13}, and it implies that CGs did not initiate these gigantic jets as they did for red sprites. Therefore, the associated ELF transients were probably generated at the fully developed stage of gigantic jets. At this stage, an electric path was set up between thundercloud and ionosphere, and current flowed through this conducting channel from the ionosphere toward the thundercloud. In this scheme, the fully developed stage behaved very similarly to the return stroke of CG lightning^{20,21}. A negative cloud-to-ionosphere (–CI) discharge would generate ELF waves with the +CG polarization observed in Japan and Antarctica. However, owing to the uncertainty in the recorder clock and possible misses of the TOGA system, there is a slight probability that some of the gigantic jets could be triggered by

+CG or a +CG occurred after the jets, and the observed ELF waves were produced by +CG and the jets.

Transient luminous events such as sprites and blue jets in the upper atmosphere have been studied extensively in the past decade^{1–14}. However, so far only six gigantic optical jets have been observed, and all were from oceanic thunderstorms. It is likely that the gigantic jets are a special feature of oceanic thunderstorms.

In a realistic model of global electric circuit¹⁶, the upper branch should be the whole atmosphere, which carries $\sim 2 \times 10^5$ C of charges. Most of the positive charges are confined to several tens of kilometres near the ground, and most of the $\sim 3 \times 10^5$ volts potential drop between the ionosphere and the ground^{15,16,20,21} also occurs in the same elevation. The traditional role of thunderstorms is to charge and to maintain the potential difference. In contrast, the gigantic jets, and possibly sprites^{17,18}, play a role in the global circuit by discharging the ionosphere and reducing the potential difference, with each jet removing ~ 30 C from the ionosphere. The charges removed by each jet account for $\sim 0.02\%$ of the total charged in the atmosphere but account for a substantial fraction of charges residing in the lower ionosphere. □

Received 2 January; accepted 27 May 2003; doi:10.1038/nature01759.

1. Franz, R. C., Nemzek, R. J. & Winckler, J. R. Television image of a large upward electrical discharge above a thunderstorm system. *Science* **249**, 48–51 (1990).
2. Sentman, D. D., Wescott, E. M., Osborne, D. L., Hampton, D. L. & Heavner, M. J. Preliminary results from the Sprites 94 aircraft campaign: 1. Red sprites. *Geophys. Res. Lett.* **22**, 1205–1208 (1995).
3. Boeck, W. L. *et al.* Observations of lightning in the stratosphere. *J. Geophys. Res.* **D 100**, 1465–1475 (1995).
4. Lyons, W. A. *et al.* Sprite observations above the U.S. High Plains in relation to their parent thunderstorm systems. *J. Geophys. Res.* **101**, 29641–29652 (1996).
5. Pasko, V. P., Inan, U. S. & Bell, T. F. Sprites as luminous columns of ionization produced by quasi-electrostatic thunderstorm fields. *Geophys. Res. Lett.* **23**, 649–652 (1996).
6. Hardman, S. F. *et al.* Sprite observations in the Northern Territory of Australia. *J. Geophys. Res.* **D 105**, 4689–4697 (2000).
7. Su, H. T., Hsu, R. R., Chen, A. B., Lee, Y. J. & Lee, L. C. Observation of sprites over the Asian continent and over oceans around Taiwan. *Geophys. Res. Lett.* **29**, 101029/2001GL013737 (2002).
8. Takahashi, Y. *et al.* Activities of sprites and elves in the winter season, Japan. *J. Atmos. Terr. Phys.* **65**, 551–560 (2003).
9. Lyons, W. A., Nelson, T. E., Armstrong, R. A., Pasko, V. P. & Stanley, M. A. Upward electrical discharges from thunderstorm tops. *Bull. Am. Meteorol. Soc.* **84**, 445–454 (2003).
10. Wescott, E. M., Sentman, D. D., Osborne, D. L., Hampton, D. L. & Heavner, M. J. Preliminary results from the Sprites 94 aircraft campaign: 2. Blue jets. *Geophys. Res. Lett.* **22**, 1209–1212 (1995).
11. Wescott, E. M. *et al.* Blue starters: Brief upward discharges from an intense Arkansas thunderstorm. *Geophys. Res. Lett.* **23**, 2153–2156 (1996).
12. Wescott, E. M., Sentman, D. D., Heavner, M. J., Hampton, D. L. & Vaughan, O. H. Blue jets: Their relationship to lightning and very large hailfall, and physical mechanisms for their production. *J. Atmos. Terr. Phys.* **60**, 713–714 (1998).
13. Wescott, E. M. *et al.* New evidence for the brightness and ionization of blue starters and blue jets. *J. Geophys. Res.* **A 106**, 21549–21554 (2001).
14. Pasko, V. P., Stanley, M. A., Mathews, J. D., Inan, U. S. & Wood, T. G. Electrical discharge from a thundercloud top to the lower ionosphere. *Nature* **416**, 152–154 (2002).
15. Roble, R. G. On modeling component processes in the Earth's global electric circuit. *J. Atmos. Terr. Phys.* **53**, 831–847 (1991).
16. Rycroft, M. J., Israelsson, S. & Price, C. The global atmospheric electric circuit, solar activity and climate change. *J. Atmos. Terr. Phys.* **62**, 1563–1576 (2000).
17. Sato, M. *et al.* Charge moment differences in winter of Japan and summer of the United States. *Eos* **83**, A11C–0103 (2002).
18. Hu, W., Cummer, S. A., Lyons, W. A. & Nelson, T. E. Lightning charge moment changes for the initiation of sprites. *Geophys. Res. Lett.* **29**, 101029/2001GL014593 (2002).
19. Bilizia, D. International Reference Ionosphere 2000. *Radio Sci.* **36**, 261–275 (2001).
20. Uman, M. A. *The Lightning Discharge* (Academic, Orlando, 1987).
21. MacGorman, D. R. & Rust, W. D. *The Electrical Nature of Storms* (Oxford Univ. Press, Oxford, 1998).
22. Landau, L. D. & Lifshitz, E. M. *Fluid Mechanics*, 2nd edn (Pergamon, Oxford, 1987).
23. Huang, E. *et al.* Criteria for sprites and elves based on Schumann resonance observations. *J. Geophys. Res.* **104**, 16943–16964 (1999).
24. Dowden, R. L., Brundell, J. B. & Rodger, C. J. VLF lightning location by time of group arrival (TOGA) at multiple sites. *J. Atmos. Terr. Phys.* **64**, 817–830 (2002).

Acknowledgements We thank R. Dowden for providing the TOGA data and for discussions. This work was supported in part by the National Space Program Office and National Science Council in Taiwan.

Competing interests statement The authors declare that they have no competing financial interests.

Correspondence and requests for materials should be addressed to H.T.S. (htsu@phys.ncku.edu.tw).

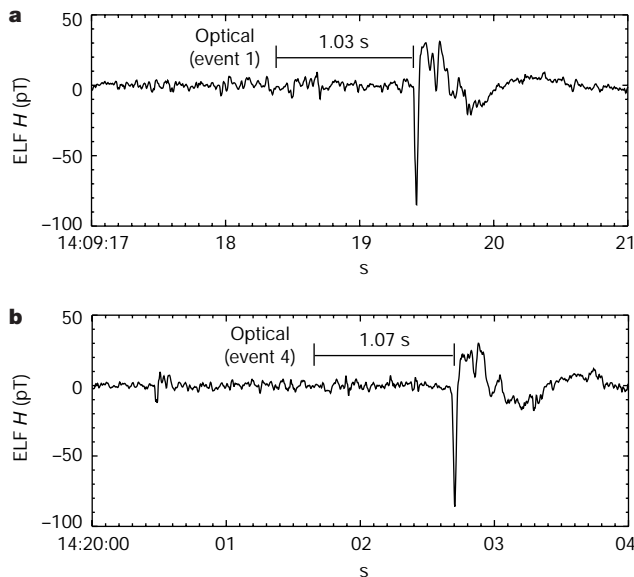


Figure 4 The *H*-component of ELF waves associated with the jets shown in Figs 2 and 3. The ELF transients were recorded at Onagowa (38.4° N, 141.5° E), Japan, on 22 July 2002.